The Astrophysical Journal, 633:603–610, 2005 November 10

CAN GAMMA-RAY BURSTS BE USED TO MEASURE COSMOLOGY? A FURTHER ANALYSIS

D. Xu,[1] Z. G. Dai,[1] and E. W. Liang[1,2,3]

Received 2004 October 29; accepted 2005 July 16

ABSTRACT

Three different methods of measuring cosmology with gamma-ray bursts (GRBs) have been proposed since a relation between the gamma-ray energy E_γ of a GRB jet and the peak energy E_p of the νF_ν spectrum in the burst frame was reported by Ghirlanda and coauthors. In method I, to calculate the probability for a favored cosmology, only the contribution of the E_γ-E_p relation that is already best-fitted for this cosmology is considered. We apply this method to a sample of 17 GRBs and obtain the mass density $\Omega_M = 0.15^{+0.45}_{-0.13}$ (1 σ) for a flat ΛCDM universe. In method II, to calculate the probability for some certain cosmology, contributions of all the possible E_γ-E_p relations that are best-fitted for their corresponding cosmologies are taken into account. With this method, we find a constraint on the mass density $0.14 < \Omega_M < 0.69$ (1 σ) for a flat universe. In method III, to obtain the probability for some cosmology, contributions of all the possible E_γ-E_p relations associated with their unequal weights are considered. With this method, we obtain an inspiring constraint on the mass density $0.16 < \Omega_M < 0.45$ (1 σ) for a flat universe and $\chi^2_{\rm dof} = 19.08/15 = 1.27$ for the concordance model of $\Omega_M = 0.27$. Compared with the previous two methods, method III makes the observed 17 GRBs place much more stringent confidence intervals at the same confidence levels. Furthermore, we perform a Monte Carlo simulation and use a larger sample to investigate the cosmographic capabilities of GRBs with different methods. We find that a larger GRB sample could be used to effectively measure cosmology, no matter whether the E_γ-E_p relation is calibrated by low-z bursts or not. Ongoing observations of GRBs in the *Swift* era are expected to make the cosmological utility of GRBs progress from its babyhood into childhood.

Subject headings: cosmology: observations — distance scale — gamma rays: bursts

1. INTRODUCTION

The traditional cosmology has been revolutionized by modern sophisticated observation techniques in distant Type Ia supernovae (SNe Ia; e.g., Riess et al. 1998; Schmidt et al. 1998; Perlmutter et al. 1999), cosmic microwave background (CMB) fluctuations (e.g., Bennett et al. 2003; Spergel et al. 2003), and large-scale structure (LSS; e.g., Allen et al. 2003; Tegmark et al. 2004). Each type of cosmological data tends to play a unique role in measuring cosmology. In modern cosmology, it has been convincingly suggested that the global mass-energy budget of the universe, and thus its dynamics, is dominated by a dark energy component and that the currently accelerating universe had once been decelerating (e.g., Riess et al. 2004). The cosmography and the nature of dark energy, as well as its evolution with redshift, are some of the most important issues in physics and astronomy today.

Gamma-ray bursts (GRBs) are the most intense explosions observed so far. They are believed to be detectable up to a very high redshift (Lamb & Reichart 2000; Ciardi & Loeb 2000; Bromm & Loeb 2002; Gou et al. 2004), and their high-energy photons are almost immune to dust extinction. These advantages would make GRBs an attractive cosmic probe.

From the isotropic equivalent peak luminosity $L_{\rm iso}$-variability (or spectral lag) relation (Fenimore & Ramirez-Ruiz 2000; Norris et al. 2000), the standard energy reservoir E_γ of GRB jets (Frail et al. 2001), the $L_{\rm iso}$–peak energy E_p of the νF_ν spectrum in the burst frame relation (Lloyd-Ronning & Petrosian 2002; Lloyd-Ronning & Ramirez-Ruiz 2002; Yonetoku et al. 2004), and the isotropic equivalent energy $E_{\rm iso}$-E_p relation (Amati et al. 2002), to the beaming-corrected energy E_γ-E_p relation (hereafter Ghirlanda relation; Ghirlanda et al. 2004a), GRBs are becoming more and more standardized candles. However, these relations in GRBs have not been calibrated by a low-z GRB sample, so one should look for a method that is different from the "classical Hubble diagram" method for SNe Ia.

The luminosity relations with the variability and spectral lag make GRBs a distance indicator in the same sense as Cepheids and SNe Ia, in which an observed light-curve property can yield an apparent distance modulus (DM). Schaefer (2003, hereafter S03) considered these two relations for nine bursts with known redshifts and advocated a new cosmographic method (hereafter method I) for GRBs. In method I, one first calibrates the two relations with the observed sample for a certain cosmology and then applies the best-fit relations back to the observed sample to obtain a χ^2 or a probability $P \propto \exp(-\chi^2/2)$ for this cosmology. Similar to the brightness of SNe Ia, the energy reservoirs in GRB jets are also clustered, but they are not fine enough for precise cosmology (Bloom et al. 2003). Amati et al. (2002) found a $E_{\rm iso} \propto E_p^k$ ($k \sim 2$) relation from 12 *BeppoSAX* bursts. The *High Energy Transient Explorer 2* (*HETE-2*) observations confirm this relation and extend it to X-ray flashes (Sakamoto et al. 2004; Lamb et al. 2004). In addition, it also holds within a GRB (Liang et al. 2004). The Ghirlanda relation is written as $(E_\gamma/10^{50}\ {\rm ergs}) = C(E_p/100\ {\rm keV})^a$, where a and C are dimensionless parameters. Theoretical explanations of this relation include the standard synchrotron mechanism in relativistic shocks (Zhang & Mészáros 2002; Dai & Lu 2002), together with the afterglow jet model, or the emission from off-axis relativistic jets (Yamazaki et al. 2004; Eichler & Levinson 2004; Levinson & Eichler 2005). This relation could also be understood as due to Comptonization of the thermal radiation flux that is advected from the base of an outflow in the dissipative photosphere model (e.g., Rees & Mészáros

[1] Department of Astronomy, Nanjing University, 22 Hankou Lu, Nanjing 210093, China.
[2] Department of Physics, Guangxi University, Nanning 530004, China.
[3] Department of Physics, University of Nevada at Las Vegas, 4505 South Maryland Parkway, Las Vegas, NV 89154.

2005). If these explanations are true, the Ghirlanda relation appears to be intrinsic. Thus, Dai et al. (2004, hereafter DLX04) considered the Ghirlanda relation for 12 bursts and proposed another cosmographic method (hereafter method II) for GRBs. In method II, one makes marginalizations over the unknown parameters in the Ghirlanda relation to obtain a χ^2 or a probability $P \propto \exp(-\chi^2/2)$ for a certain cosmology. Following Schaefer's method, Ghirlanda et al. (2004b, hereafter GGLF04) and Friedman & Bloom (2005, hereafter FB05) also investigated the same issue but used different GRB data. Recently, Firmani et al. (2005, hereafter FGGA05) considered the Ghirlanda relation for 15 bursts and proposed a Bayesian approach for their cosmological use (hereafter method III). In method III, to obtain the probability for a certain cosmology, one considers contributions of all the possible E_γ-E_p relations associated with their unequal weights. The detailed procedures of the three methods are shown in § 2.1, and they indicate that method III is the optimal one.

As analyzed previously, due to the lack of low-z GRBs, methods I, II, and III are different from the classical Hubble diagram method for SNe Ia. In this paper, we investigate the constraints on cosmological parameters from the observed 17 GRBs with different methods. Because the present GRB sample is a small one, it is necessary to use a large simulated sample, which may be established in the *Swift* era, to discuss the cosmographic capabilities with different methods.

This paper is arranged as follows. In § 2, we describe our analytical methods and data. The results from the observed GRB sample are presented in § 3. In § 4, we perform Monte Carlo simulations and analyze the results from the simulated GRB sample. Conclusions and discussion are presented in § 5.

2. METHOD AND SAMPLE ANALYSIS

2.1. *Method Analysis*

According to the relativistic fireball model, the emission from a spherically expanding shell and that from a jet are similar to each other if the observer is along the jet's axis and the Lorentz factor of the fireball is larger than the inverse of the jet's half-opening angle θ, but when the Lorentz factor drops below θ^{-1}, the jet's afterglow light curve is expected to present a break because of the edge effect and the laterally spreading effect (Rhoads 1999; Sari et al. 1999). Therefore, together with the assumptions of the initial fireball emitting a constant fraction η_γ of its kinetic energy into prompt gamma rays and a constant circumburst particle density n, the jet's half-opening angle is derived to be

$$\theta = 0.163 \left(\frac{t_{j,d}}{1+z}\right)^{3/8} \left(\frac{n_0}{E_{\rm iso,52}} \frac{\eta_\gamma}{1-\eta_\gamma}\right)^{1/8}, \quad (1)$$

where $E_{\rm iso,52} = E_{\rm iso}/10^{52}$ ergs, $t_{j,d} = t_j/1$ day, and $n_0 = n/1\ {\rm cm}^{-3}$. The "bolometric" isotropic equivalent gamma-ray energy of a GRB is given by

$$E_{\rm iso} = \frac{4\pi d_L^2 S_\gamma k}{1+z}, \quad (2)$$

where S_γ is the fluence (in units of ergs cm^{-2}) received in an observed bandpass and the quantity k is a multiplicative correction of order unity relating the observed bandpass to a standard rest-frame bandpass (1–10^4 keV in this paper; Bloom et al. 2001). The energy release of a GRB jet is thus given by

$$E_\gamma = (1-\cos\theta) E_{\rm iso}, \quad (3)$$

where the fractional uncertainty (FB05) is

$$\left(\frac{\sigma_{E_\gamma}}{E_\gamma}\right)^2 = \left(1-\sqrt{C_\theta}\right)^2 \left[\left(\frac{\sigma_{S_\gamma}}{S_\gamma}\right)^2 + \left(\frac{\sigma_k}{k}\right)^2\right] + C_\theta \left[\left(\frac{3\sigma_{t_j}}{t_j}\right)^2 + \left(\frac{\sigma_{n_0}}{n_0}\right)^2 + \left(\frac{\sigma_{\eta_\gamma}}{\eta_\gamma - \eta_\gamma^2}\right)^2\right], \quad (4)$$

where

$$C_\theta = \left(\frac{\theta \sin\theta}{8 - 8\cos\theta}\right)^2. \quad (5)$$

The Ghirlanda relation is

$$\frac{E_\gamma}{10^{50}\ {\rm ergs}} = C \left(\frac{E_p}{100\ {\rm keV}}\right)^a, \quad (6)$$

where a and C are assumed to have no covariance and $E_p = E_p^{\rm obs}(1+z)$. Combining equations (1)–(3) and (6), we derive the apparent luminosity distance with the small-angle approximation (i.e., $\theta \ll 1$)[4] as

$$d_L = 7.575 \frac{(1+z) C^{2/3} [E_p^{\rm obs}(1+z)/100\ {\rm keV}]^{2a/3}}{(k S_\gamma t_{j,d})^{1/2} (n_0 \eta_\gamma)^{1/6}}\ {\rm Mpc}. \quad (7)$$

Assuming that all the observables are independent of each other and their errors satisfy Gaussian distributions, we derive the fractional uncertainty of the apparent luminosity distance without the small-angle approximation,

$$\left(\frac{\sigma_{d_L}}{d_L}\right)^2 = \frac{1}{4}\left[\left(\frac{\sigma_{S_\gamma}}{S_\gamma}\right)^2 + \left(\frac{\sigma_k}{k}\right)^2\right] + \frac{1}{4}\frac{1}{\left(1-\sqrt{C_\theta}\right)^2}\left[\left(\frac{\sigma_C}{C}\right)^2 + \left(a\frac{\sigma_{E_p^{\rm obs}}}{E_p^{\rm obs}}\right)^2 + \left(a\frac{\sigma_a}{a}\ln\frac{E_p}{100}\right)^2\right] + \frac{1}{4}\frac{C_\theta}{\left(1-\sqrt{C_\theta}\right)^2}\left\{\left(\frac{3\sigma_{t_j}}{t_j}\right)^2 + \left(\frac{\sigma_{n_0}}{n_0}\right)^2 + \left[\frac{\sigma_{\eta_\gamma}}{\eta_\gamma(1-\eta_\gamma)}\right]^2\right\}. \quad (8)$$

For simplicity, we consider $\eta_\gamma = 0.2$ and $\sigma_{\eta_\gamma} = 0$ throughout this paper (Frail et al. 2001). The apparent DM of a burst can be given by

$$\mu_{\rm obs} = 5\log d_L + 25, \quad (9)$$

with the uncertainty of

$$\sigma_{\mu_{\rm obs}} = \frac{5}{\ln 10}\frac{\sigma_{d_L}}{d_L}. \quad (10)$$

[4] This approximation is valid because $|(1-\cos\theta-\theta^2/2)/(1-\cos\theta)| < 1\%$ when $\theta < 0.35$ rad and $<0.4\%$ when $\theta < 0.22$ rad.

On the other hand, the theoretical luminosity distance in Λ models (Carroll et al. 1992) is given by

$$d_L = c(1+z)H_0^{-1}|\Omega_k|^{-1/2}\,\mathrm{sinn}\left\{|\Omega_k|^{1/2} \times \int_0^z dz\left[(1+z)^2(1+\Omega_M z) - z(2+z)\Omega_\Lambda\right]^{-1/2}\right\}, \quad (11)$$

where $\Omega_k = 1 - \Omega_M - \Omega_\Lambda$ and "sinn" is sinh for $\Omega_k > 0$ and sin for $\Omega_k < 0$. For $\Omega_k = 0$, equation (11) degenerates to $c(1+z)H_0^{-1}$ times the integral.

Usually, the likelihood for the parameters Ω_M and Ω_Λ can be determined from a χ^2 statistic, where

$$\chi^2(\Omega_M, \Omega_\Lambda, a, C|h) = \sum_k \left[\frac{\mu_{\rm th}(z_k;\Omega_M,\Omega_\Lambda|h) - \mu_{\rm obs}(z_k;\Omega_M,\Omega_\Lambda,a,C|h)}{\sigma_{\mu_{\rm obs}(z_k;\Omega_M,\Omega_\Lambda,a,C,\sigma_a/a,\sigma_C/C)}}\right]^2, \quad (12)$$

where the dimensionless Hubble constant $h \equiv H_0/100$ km s^{-1} Mpc^{-1} is taken as 0.71. If the Ghirlanda relation could be calibrated by low-z bursts, the above χ^2 statistic becomes the same as that in SNe Ia, that is,

$$\chi^2(\Omega_M, \Omega_\Lambda, h) = \sum_k \left[\frac{\mu_{\rm th}(z_k;\Omega_M,\Omega_\Lambda,h) - \mu_{{\rm obs},k}}{\sigma_{\mu_{{\rm obs},k}}}\right]^2, \quad (13)$$

where h should be marginalized.

The procedures of methods I, II, and III are as follows.

Method I (see S03; GGLF04; FB05).—The procedure of this method is to (1) fix $\Omega_i \equiv (\Omega_M, \Omega_\Lambda)_i$, (2) calculate $\mu_{\rm th}$ and E_γ for each burst for that cosmology, (3) best fit the E_γ-E_p relation to yield $(a, C)_i$ and $(\sigma_a/a, \sigma_C/C)_i$, (4) substitute $(a, C)_i$ and $(\sigma_a/a, \sigma_C/C)_i$ into equations (7) and (8) and thus derive $\mu_{\rm obs}$ and $\sigma_{\mu_{\rm obs}}$ for each burst for cosmology Ω_i, (5) calculate χ^2 for cosmology Ω_i by comparing $\mu_{\rm th}$ with $\mu_{\rm obs}$ and $\sigma_{\mu_{\rm obs}}$ and then convert it to the probability by $P(\Omega_i) \propto \exp[-\chi^2(\Omega_i)/2]$ (Riess et al. 1998), and (6) repeat steps 1–5 from $i = 1$ to N to obtain the probability for each cosmology. Therefore, method I is formulized by

$$P(\Omega_i) = P(\Omega_i|\Omega_i), \quad i = 1, N. \quad (14)$$

Method II (see DLX04).—The procedure of this method is to (1) fix Ω_i, (2) calculate $\mu_{\rm th}$ and E_γ for each burst for that cosmology, (3) best fit the E_γ-E_p relation to yield $(a, C)_i$ and $(\sigma_a/a, \sigma_C/C)_i$, (4) substitute $(a, C)_i$ and $(\sigma_a/a, \sigma_C/C)_i$ into equations (7) and (8) and thus derive $\mu_{\rm obs}$ and $\sigma_{\mu_{\rm obs}}$ for each burst for cosmology Ω_i, (5) repeat steps 1–4 from $i = 1$ to N to obtain $\mu_{\rm th}$, $\mu_{\rm obs}$, and $\sigma_{\mu_{\rm obs}}$ for each burst for each cosmology, (6) refix Ω_j, (7) calculate $\chi^2(\Omega_j|\Omega_i)$ by comparing $\mu_{\rm th}(\Omega_j)$ with $\mu_{\rm obs}(\Omega_i)$ and $\sigma_{\mu_{\rm obs}}(\Omega_i)$ and then convert it to a conditional probability by $P(\Omega_j|\Omega_i) \propto \exp\left[-\chi^2(\Omega_j|\Omega_i)/2\right]$, (8) repeat step 7 from $i = 1$ to N to obtain the probability for cosmology Ω_j by $P(\Omega_j) \propto \sum_i \exp\left[-\chi^2(\Omega_j|\Omega_i)/2\right]$, and (9) repeat steps 6–8 from $j = 1$ to N to obtain the probability for each cosmology. Method II is described by

$$P\left(\Omega_j\right) = \sum_{i=1}^{N} P\left(\Omega_j|\Omega_i\right), \quad j = 1, N. \quad (15)$$

Method III (see FGGA05).—Method III is an improvement of method II. Its key idea is to consider unequal weights for different E_γ-E_p relations, i.e., unequal weights for different conditional probabilities $P(\Omega_j|\Omega_i)$. Therefore, the first seven steps of this method are the same as those of method II. The follow-up procedure is to (8) repeat step 7 from $i = 1$ to N to obtain an iterative probability for cosmology Ω_j by $P^{\rm ite}(\Omega_j) \propto \sum_i \exp\left[-\chi^2(\Omega_j|\Omega_i)/2\right] P^{\rm ini}(\Omega_i)$ [here the initial probability $P^{\rm ini}(\Omega)$ for each cosmology is regarded as equal; e.g., $P^{\rm ini}(\Omega) \equiv 1$], (9) repeat steps 6–8 from $j = 1$ to N to obtain an iterative probability $P^{\rm ite}(\Omega)$ for each cosmology, (10) replace $P^{\rm ini}(\Omega)$ in step 8 with $P^{\rm ite}(\Omega)$ in step 9, then repeat steps 8–9, and thus reach another set of iterative probabilities for each cosmology, and (11) run the above cycle again and again until the probability for each cosmology converges, i.e., $P^{\rm ite}(\Omega) \Rightarrow P^{\rm fin}(\Omega)$ after tens of cycles.

In this method, to calculate the probability $P^{\rm fin}(\Omega_j)$ for a favored cosmology, we consider contributions of all the possible E_γ-E_p relations associated with their weights. The conditional probability $P(\Omega_j|\Omega_i)$ denotes the contribution of some certain relation, and $P^{\rm fin}(\Omega_i)$ weights the likelihood of this relation for its corresponding cosmology. Therefore, the Bayesian approach can be formulized by

$$P^{\rm fin}\left(\Omega_j\right) = \sum_{i=1}^{N} P\left(\Omega_j|\Omega_i\right) P^{\rm fin}(\Omega_i), \quad j = 1, N. \quad (16)$$

However, FGGA05 took different calculations for the conditional probability $P(\Omega_j|\Omega_i)$. Making use of the incomplete gamma function, they transformed $\chi^2(\Omega_j|\Omega_i)$ into its corresponding conditional probability $P(\Omega_j|\Omega_i)$. Actually, once the parameters $(a, C)_i$ and $(\sigma_a/a, \sigma_C/C)_i$ of the Ghirlanda relation are calibrated for cosmology Ω_i, they become "known" for the cosmic model Ω_j. So herein the meaning of $\chi^2(\Omega_j|\Omega_i)$ is the same as that for SNe Ia. In this paper, we redefine the conditional probability $P(\Omega_j|\Omega_i)$ by the formula $P(\Omega_j|\Omega_i) \propto \exp\left[-\chi^2(\Omega_j|\Omega_i)/2\right]$.

2.2. *Sample Analysis*

The great diversity in GRB phenomena suggests that the GRB population may consist of substantially different subclasses (e.g., MacFadyen & Woosley 1999; Bloom et al. 2003; Sazonov et al. 2004; Soderberg et al. 2004). To make GRBs a standard candle, a homogenous GRB sample is required. The most prominent observational evidence for a GRB jet is its temporal break in their afterglow light curves. For some bursts, e.g., GRB 030329, their temporal breaks are observed in both optical and radio bands. Berger et al. (2003) argued that these two breaks are caused by the narrow component and the wide component of the jet in this burst, respectively, indicating that the physical origins of the breaks in the optical band and in the radio band are different. In addition, the radio afterglow light curves fluctuate significantly. For example, in the case of GRB 970508, the light curve of its radio afterglow does not clearly present a break. Only a lower limit of $t_j > 25$ days was proposed by Frail et al. (2000). Furthermore, the light curve of its optical afterglow is proportional to $t^{-1.1}$, in which case no break appears (Galama et al. 1998). We thus include in our analysis only those bursts whose temporal breaks in their optical afterglow light curves were well measured. We obtain a sample of 17 GRBs, excluding GRB 970508. They are listed in Table 1.

We correct the observed fluence in a given bandpass to a "bolometric" bandpass of $1–10^4$ keV with spectral parameters. The fluence and spectral parameters for a burst fitted by different

TABLE 1
SAMPLE OF 17 GRBs

GRB	z	$E_p^{\rm obs}(\sigma_{E_p}^{\rm obs})$[a] (keV)	$[\alpha, \beta]$[a]	$S_\gamma(\sigma_{S_\gamma})$[b] ($10^{-6}$ ergs cm^{-2})	Bandpass[b] (keV)	$t_j(\sigma_{t_j})$[c] (days)	n (σ_n)[d] (cm^{-3})	η_γ[e]	References[f]	Detected by
GRB 970828.....	0.9578	297.7 [59.5]	−0.70, −2.07	96.0 [9.6]	20–2000	2.2 (0.4)	3.0 [2.4]	0.2	1, 2, 2, 3, 1, none	BATSE
GRB 980703.....	0.966	254.0 [50.8]	−1.31, −2.40	22.6 [2.26]	20–2000	3.4 (0.5)	28.0 (10.0)	0.2	4, 2, 2, 3, 5, 5	BATSE
GRB 990123.....	1.600	780.8 (61.9)	−0.89, −2.45	300.0 (40.0)	40–700	2.04 (0.46)	3.0 [2.4]	0.2	6, 7, 7, 7, 6, none	*BeppoSAX*
GRB 990510.....	1.619	161.5 (16.0)	−1.23, −2.70	19.0 (2.0)	40–700	1.57 (0.03)	0.29 (0.14)	0.2	8, 7, 7, 7, 9, 10	*BeppoSAX*
GRB 990705.....	0.8424	188.8 (15.2)	−1.05, −2.20	75.0 (8.0)	40–700	1.0 (0.2)	3.0 [2.4]	0.2	11, 7, 7, 7, 12, none	*BeppoSAX*
GRB 990712.....	0.4331	65.0 (10.5)	−1.88, −2.48	6.5 (0.3)	40–700	1.6 (0.2)	3.0 [2.4]	0.2	8, 7, 7, 7, 13, none	*BeppoSAX*
GRB 991216.....	1.020	317.3 [63.4]	−1.23, −2.18	194.0 [19.4]	20–2000	1.2 (0.4)	4.7 (2.8)	0.2	14, 2, 2, 3, 15, 10	BATSE
GRB 011211.....	2.140	59.2 (7.6)	−0.84, −2.30	5.0 [0.5]	40–700	1.56 (0.02)	3.0 [2.4]	0.2	16, 17, 17, 3, 18, none	*BeppoSAX*
GRB 020124.....	3.200	120.0 (22.6)	−1.10, −2.30	6.8 [0.68]	30–400	3.0 (0.4)	3.0 [2.4]	0.2	19, 20, 20, 20, 21, none	*HETE-2*
GRB 020405.....	0.690	192.5 (53.8)	0.00, −1.87	74.0 (0.7)	15–2000	1.67 (0.52)	3.0 [2.4]	0.2	22, 22, 22, 22, 22, none	*BeppoSAX*
GRB 020813.....	1.255	212.0 (42.0)	−1.05, −2.30	102.0 [10.2]	30–400	0.43 (0.06)	3.0 [2.4]	0.2	23, 20, 20, 20, 23, none	*HETE-2*
GRB 021004.....	2.332	79.8 (30.0)	−1.01, −2.30	2.55 (0.60)	2–400	4.74 (0.14)	30.0 (27.0)	0.2	24, 25, 25, 25, 26, 27	*HETE-2*
GRB 021211.....	1.006	46.8 (5.5)	−0.805, −2.37	2.17 (0.15)	30–400	1.4 (0.5)	3.0 [2.4]	0.2	28, 29, 29, 29, 30, none	*HETE-2*
GRB 030226.....	1.986	97.1 (20.0)	−0.89, −2.30	5.61 (0.65)	2–400	1.04 (0.12)	3.0 [2.4]	0.2	31, 25, 25, 25, 32, none	*HETE-2*
GRB 030328.....	1.520	126.3 (13.5)	−1.14, −2.09	36.95 (1.40)	2–400	0.8 (0.1)	3.0 [2.4]	0.2	33, 25, 25, 25, 34, none	*HETE-2*
GRB 030329.....	0.1685	67.9 (2.2)	−1.26, −2.28	110.0 (10.0)	30–400	0.48 (0.03)	1.0 (0.11)	0.2	35, 36, 36, 36, 37, 38	*HETE-2*
XRF 030429	2.658	35.0 (9.0)	−1.12, −2.30	0.854 (0.14)	2–400	1.77 (1.0)	3.0 [2.4]	0.2	39, 25, 25, 25, 39, none	*HETE-2*

[a] The spectral parameters fitted by the Band function. The fractional uncertainties of $E_p^{\rm obs}$ are taken as 20% when not reported, and the fractional uncertainty of the k-correction is fixed at 5%.

[b] The fluences and their errors in the observed energy band. The fractional errors are taken as 10% when not reported. The fluence and spectral parameters of a GRB are selected from the same original literature if possible. If this criterion is unsatisfied, fluences are chosen in the widest energy band.

[c] Afterglow break times and errors in the optical band.

[d] The circumburst densities and errors from broadband modeling of the afterglow light curves. If not available, the value of n is taken as 3.0 ± 2.4 cm^{-3}.

[e] The constant efficiency η_γ of converting explosion energy into gamma-ray emission for each burst.

[f] References are in the following order: z, $E_p^{\rm obs}$, $[\alpha, \beta]$, S_γ, t_j, n.

REFERENCES.—(1) Djorgovski et al. 2001; (2) Jimenez et al. 2001; (3) Bloom et al. 2003; (4) Djorgovski et al. 1998; (5) Frail et al. 2003; (6) Kulkarni et al. 1999; (7) Amati et al. 2002; (8) Vreeswijk et al. 2001; (9) Stanek et al. 1999; (10) Panaitescu & Kumar 2002; (11) Le Floc'h et al. 2002; (12) Masetti et al. 2000; (13) Björnsson et al. 2001; (14) Piro et al. 2000; (15) Halpern et al. 2000; (16) Holland et al. 2002; (17) Amati 2003; (18) Jakobsson et al. 2003; (19) Hjorth et al. 2003; (20) Barraud et al. 2003; (21) Berger et al. 2002; (22) Price et al. 2003a; (23) Barth et al. 2003; (24) Matheson et al. 2003; (25) Sakamoto et al. 2005; (26) Holland et al. 2003; (27) Schaefer et al. 2003; (28) Vreeswijk et al. 2003; (29) Crew et al. 2003; (30) Holland et al. 2004; (31) Greiner et al. 2003a; (32) Klose et al. 2004; (33) Rol et al. 2003; (34) Andersen et al. 2003; (35) Greiner et al. 2003b; (36) Vanderspek et al. 2004; (37) Price et al. 2003b; (38) Tiengo et al. 2003; (39) Jakobsson et al. 2004.

authors may be affected by different criteria (or systematic biases) in their works. We thus collect a couple of fluence and spectral parameters from the same original literature. For GRB 970828, GRB 980703, GRB 991216, and GRB 011211, the fluence and spectral parameters are unavailable in the same original literature, so we choose their fluences measured in the widest energy band available in the other literature.

For GRB 011211, we approximately take the high-energy spectral index β to be -2.3 because it is unreported in Amati (2003). The spectra of *HETE-2*–detected GRB 020124, GRB 020813, GRB 021004, GRB 030226, and XRF 030429 are not fitted by the Band function but by the cutoff power-law model (Band et al. 1993). However, it is appropriate that their corresponding "bolometric" fluences are calculated by the former model with $\beta \sim -2.3$, avoiding the potential systematic bias that is brought by applying different spectral models for one observed sample (Barraud et al. 2003).

The circumburst densities of several bursts in our sample have been obtained from broadband modeling of the afterglow emission (e.g., Panaitescu & Kumar 2002). For the bursts with unknown n, we assumed $n \simeq 3$ cm^{-3} as the median value of the distribution of the measured densities, together with a constant fractional uncertainty of 80% (Ghirlanda et al. 2004a; DLX04).

3. COSMOLOGICAL CONSTRAINTS

We first fit the E_γ-E_p relation for the cosmology of $\Omega_M = 0.27$, $\Omega_\Lambda = 0.73$, and $h = 0.71$ and obtain $a = 1.53$, $C = 0.97$, $\sigma_a/a = 0.05$, and $\sigma_C/C = 0.08$, together with $\chi^2_\nu = 21.93/15.0 = 1.46$, using equation (4) for the estimation of $\sigma_{E_\gamma}/E_\gamma$ (Press et al. 1999, p. 660). Substituting the best-fit results into equations (7) and (8), we plot the Hubble diagram for the observed GRB sample in the concordance model of $\Omega_M = 0.27$, which is shown in Figure 1 (*filled circles*). Shown for comparison are the Hubble diagrams for the binned gold sample of SNe Ia (*open circles*;

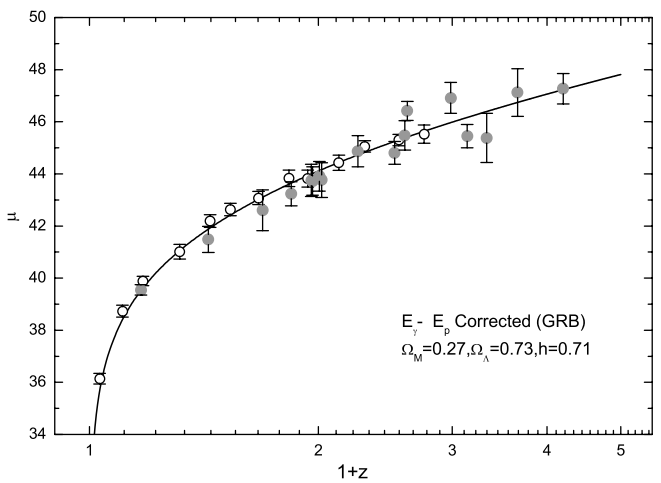

FIG. 1.—Hubble diagrams for the observed GRB sample (*filled circles*) and for the binned gold sample of SNe Ia (*open circles*). The GRB E_γ-E_p relation has been calibrated in the cosmic model of $\Omega_M = 0.27$, $\Omega_\Lambda = 0.73$, and $h = 0.71$ (*solid line*).

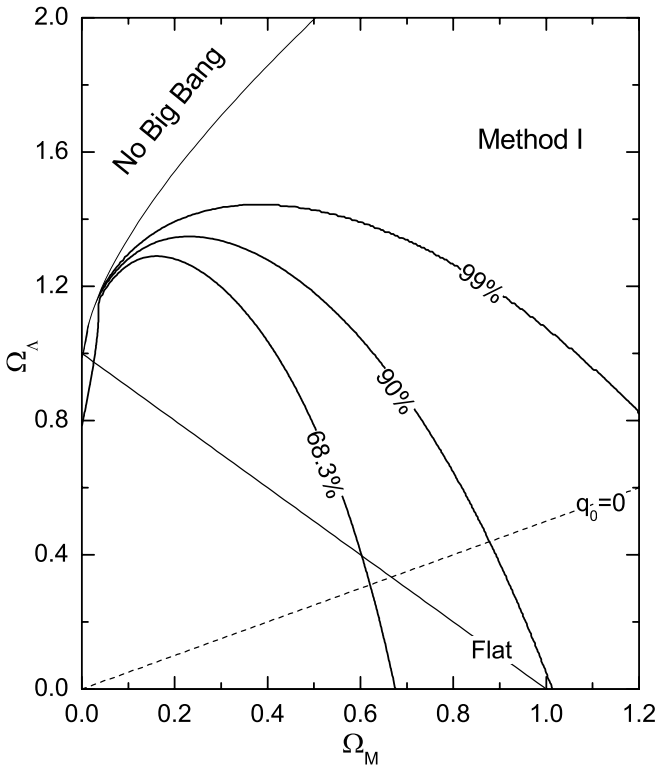

FIG. 2.—Joint confidence intervals (68.3%, 90%, and 99%) in the Ω_M-Ω_Λ plane from the 17 GRBs with method I.

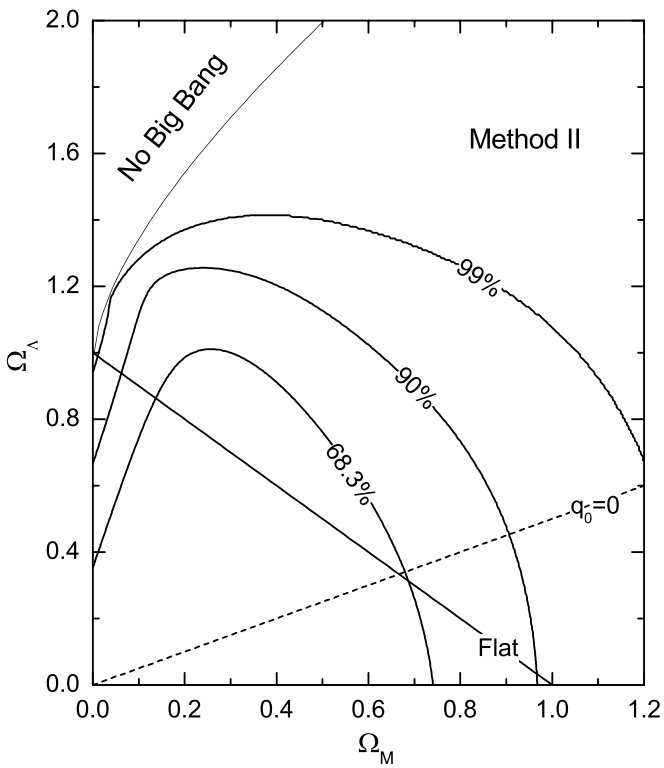

FIG. 3.—Same as Fig. 2, but with method II.

Riess et al. 2004) and the theoretical model of $\Omega_M = 0.27$ and $\Omega_\Lambda = 0.73$ (*solid line*).

The constraints with method I are shown in Figure 2 (*solid contours*). In the concordance model of $\Omega_M = 0.27$, we find $\chi^2_{\rm dof} = 17.91/15 = 1.19$. We measure $\Omega_M = 0.15^{+0.45}_{-0.13}$ ($1\ \sigma$) for a flat ΛCDM universe. DLX04 proposed method II based on the principle that if there are unknown cosmology-independent parameters in the χ^2 statistic, they are usually marginalized over (i.e., integrating the parameters according to their probability distribution). Note that DLX04 let the parameter a of the Ghirlanda relation intrinsically equal 1.50. For the purpose of universality, in this paper we let it vary freely, similar to the parameter C of this relation (see details in § 2.1). The constraints with method II are shown in Figure 3 (*solid contours*). This method provides a more stringent constraint of $0.14 < \Omega_M < 0.69$ ($1\ \sigma$) for a flat universe.

By method I, we recalibrate the Ghirlanda relation for each cosmology, i.e., Ω_M and Ω_Λ taken from 0 to 1. We find that the half-opening angles of all the bursts are less than 0.23 rad and that the mean σ_a/a and σ_C/C are 0.049 and 0.083, respectively. As a result, the typical error terms in equation (8) are $\sigma_{S_\gamma}/2S_\gamma \sim 0.052$, $\sigma_k/2k \sim 0.025$, $[C_\theta^{1/2}/(2 - 2C_\theta^{1/2})](3\sigma_{t_j}/t_j) \sim 0.091$, $[C_\theta^{1/2}/(2 - 2C_\theta^{1/2})](\sigma_{n_0}/n_0) \sim 0.118$, $[1/(2 - 2C_\theta^{1/2})](\sigma_C/C) \sim 0.055$, $a[1/(2 - 2C_\theta^{1/2})](\sigma_{E_p^{\rm obs}}/E_p^{\rm obs}) \sim 0.168$, and $\sigma_a[1/(2 - 2C_\theta^{1/2})]|\ln [E_p^{\rm obs}(1 + z)100]| \sim 0.056$. These error terms give a typical uncertainty of apparent DM of $\sigma_{\mu_{\rm obs}} \sim 0.5$ mag, which is a factor of ~2 larger than that derived from the SN Ia gold sample.

FGGA05 proposed the Bayesian approach to use GRBs as cosmic rulers. In our work, we redefined the conditional probability in their method, called "method III" in this paper. The constraints on cosmological parameters with this method are shown in Figure 4 (*solid contours*). Compared with the previous two methods, method III does give much more stringent confidence intervals at the same confidence levels (CLs). The results are inspiring and demonstrate the advantages of high-z distance indicators in constraining cosmological parameters. The data set is consistent with the concordance model of $\Omega_M = 0.27$, yielding $\chi^2_{\rm dof} = 19.08/15 = 1.27$. We also find $0.16 < \Omega_M < 0.45$ ($1\ \sigma$) for a flat universe.

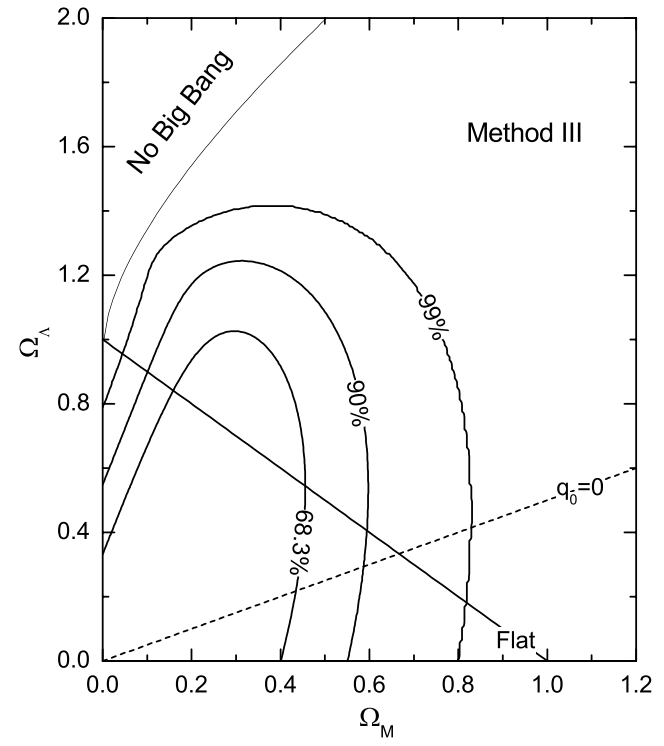

FIG. 4.—Same as Fig. 2, but with method III.

4. SIMULATIONS AND COSMOLOGICAL CONSTRAINTS

4.1. *Procedure of Simulations*

As discussed above, the method for GRB cosmology is different from that for SN cosmology due to the lack of the low-z calibration. The low-z calibration will greatly enhance the cosmographic capability of GRBs (assuming no cosmic evolution for the Ghirlanda relation). Therefore, one can ask, could a large high-z GRB sample effectively measure cosmology? To answer this question, we carry out a Monte Carlo simulation and use a large simulated sample to investigate the cosmographic capabilities in different scenarios.

Our simulations are based on the Ghirlanda relation, which is calibrated for $\Omega_M = 0.27$ and $\Omega_\Lambda = 0.73$. Making use of the sample in Table 1, we find $a = 1.53$, $C = 0.97$, $\theta < 0.2$ rad, and $\log(E_\gamma/1\ \mathrm{erg}) \in [49.82, 51.96]$. We also find $\log(E_p^{\mathrm{obs}}/1\ \mathrm{keV}) \in [1.54, 2.89]$. These restrictive conditions are imposed on our simulations. Each simulated GRB is characterized by a set of S_b', t_j', n', z, and E_p', where S_b' is the bolometric fluence.

The simulation procedure is as follows:

1. We consider the lognormal distributions for the observables S_b, t_j, and n. From the 17 GRBs, we find $\langle \log(S_b/1\ \mathrm{erg\ cm^{-2}}) \rangle \sim -4.46$ with $\sigma_{\log(S_b/1\ \mathrm{erg\ cm^{-2}})} \sim 0.78$ and $\langle \log(t_j/1\ \mathrm{day}) \rangle \sim 0.17$ with $\sigma_{\log(t_j/1\ \mathrm{day})} \sim 0.27$. Because n is unavailable in the literature for most GRBs, we take $\langle \log(n/1\ \mathrm{cm^{-3}}) \rangle \sim 0.40$ with $\sigma_{\log(n/1\ \mathrm{cm^{-3}})} \sim 0.25$. The observable z is selected according to its observational distribution cut by an upper limit $z \sim 4.5$, which is shown in Figure 5. The uncertainty of z is ignored.

2. We also consider the lognormal distributions for the fractional uncertainties of the observables S_b, t_j, n, and E_p. From the observed sample, we find $\langle \log(\sigma_{S_b}/S_b) \rangle \sim -0.97$ with $\sigma_{\log(\sigma_{S_b}/S_b)} \sim 0.16$, $\langle \log(\sigma_{t_j}/t_j) \rangle \sim -0.91$ with $\sigma_{\log(\sigma_{t_j}/t_j)} \sim 0.45$, $\langle \log(\sigma_n/n) \rangle \sim -0.30$ with $\sigma_{\log(\sigma_n/n)} \sim 0.10$, and $\langle \log(\sigma_{E_p}/E_p) \rangle \sim -0.83$ with $\sigma_{\log(\sigma_{E_p}/E_p)} \sim 0.26$, respectively. We ensure in code that the fractional uncertainties of the observables S_b, t_j, n, and E_p are less than 25%, 35%, 100%, and 35%, respectively.

3. We simulate a GRB characterized by a set of ($S_b \pm \sigma_{S_b}$, $t_j \pm \sigma_{t_j}$, $n \pm \sigma_n$, z) according to the distributions that these parameters follow, compute its E_γ in the cosmic model of $\Omega_M = 0.27$ and $\Omega_\Lambda = 0.73$, and then calculate its E_p by the Ghirlanda relation of $(E_\gamma/10^{50}\ \mathrm{ergs}) = 0.97(E_p/100\ \mathrm{keV})^{1.53}$.

4. The GRB generated in step (3) follows the "rigid" Ghirlanda relation. We add a random deviation to each parameter, except for z, to make this burst more realistic, i.e., $S_b' = S_b + 1.1(-1)^m\sigma_{S_b}$, $t_j' = t_j + 1.1(-1)^m\sigma_{t_j}$, $n' = n + 1.1(-1)^m\sigma_n$, and $E_p' = E_p + 1.1(-1)^m\sigma_{E_p}$, where m is randomly taken from 0 and 1.

5. Using the parameters S_b', t_j', n', z, and E_p', we compute the parameters θ' and E_γ' for $\Omega_M = 0.27$, $\Omega_\Lambda = 0.73$ and the quantity $E_p'^{\mathrm{obs}} = E_p'/(1+z)$.

6. Since $\theta < 0.2$ rad and $\log(E_\gamma/1\ \mathrm{erg}) \in [49.82, 51.96]$ and $\log(E_p^{\mathrm{obs}}/1\ \mathrm{keV}) \in [1.54, 2.89]$ are valid for the observed sample, we require that θ', $\log(E_\gamma'/1\ \mathrm{erg})$, and $\log(E_p'^{\mathrm{obs}}/1\ \mathrm{keV})$ of a simulated GRB must be within the corresponding ranges.

7. Repeat steps (3)–(6) to generate a sample of 80 bursts.

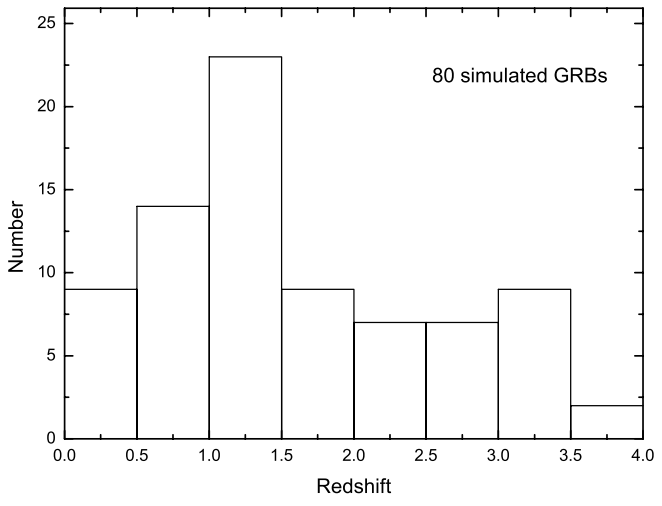

FIG. 5.—Histogram for the redshifts of 80 simulated GRBs, following the redshift distribution of the GRBs observed so far.

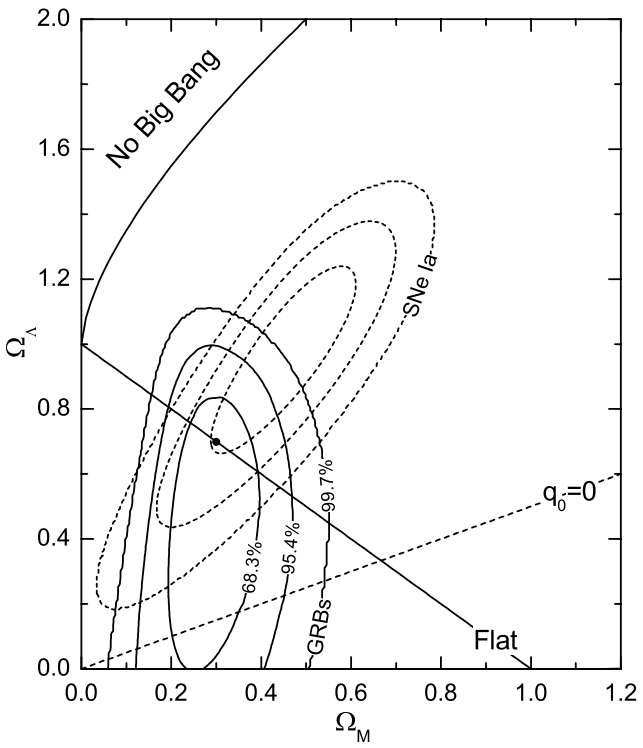

FIG. 6.—Joint confidence intervals (68.3%, 95.4%, and 99.7%) in the Ω_M-Ω_Λ plane from the 80 simulated GRBs in this work (*solid contours*) and from the 157 SNe Ia in Riess et al. (2004; *dashed contours*). The filled circle marks $\Omega_M = 0.30$ and $\Omega_\Lambda = 0.70$.

The half-opening angles of the simulated sample are less than 0.23 rad when Ω_M and Ω_Λ are taken from 0 to 1, as in the observed sample. We carry out a circular operation to achieve the simulated sample, which may be established in the *Swift* era.

4.2. *Constraints from Simulated GRBs*

By method I, we find that the typical σ_a/a and σ_C/C for the large sample decrease to 0.02 and 0.05. This is because for the small observed sample, the dispersion of the Ghirlanda relation is mainly contributed by a few "outliers," while for the large simulated sample, the bursts are distributed around the "rigid" Ghirlanda relation with a Gaussian distribution (see § 4.1). Such a large sample seems to be more realistic.

Among several scenarios, we only perform to what degree the simulated sample can constrain the Ω_M-Ω_Λ parameters with method III. The results are shown by solid confidence intervals in Figure 6. Also shown are the constraints derived from the SN gold sample (*dashed contours*) at the same CLs. The main points revealed by this figure are as follows: (1) A large high-z GRB sample could effectively measure cosmology. The simulated GRB data are consistent with the concordance model of $\Omega_M \approx 0.3$,

yielding $\chi^2_{\rm dof} = 94./78. \approx 1.20$. With the prior of a flat universe, the mass density is $\Omega_M = 0.30^{+0.09}_{-0.06}$ at the 68.3% level. (2) GRBs can better constrain Ω_M than Ω_Λ due to their high redshifts. The orientation of the elliptical contours is almost vertical to the Ω_M axis. This is an advantage of GRBs over SNe Ia for cosmological use. (3) GRBs supply complementary content to SN cosmology. The 157 SNe Ia provide evidence of cosmic acceleration at a very high CL. A large GRB sample would reach a similar conclusion. Alone the SN sample nearly rules out the flat universe model at 1 σ level, but a combination of GRBs and SNe makes the concordance model of $\Omega_M \approx 0.3$ more favored and thus in more agreement with the conclusion from *Wilkinson Microwave Anisotropy Probe* (*WMAP*) observations (Spergel et al. 2003).

If the low-z calibration is realized for GRBs, then the solid confidence regions in Figure 6 will become smaller so that they lie in the part of cosmic acceleration at a high CL in the Ω_M-Ω_Λ plane (not shown in this work). We here present a rough estimation of the detection rate of low-z bursts in the *Swift* era. Taking $\Omega_M = 0.27$, $\Omega_\Lambda = 0.73$, and $h = 0.71$, the observed rate of bursts with redshift less than z is

$$\frac{dN}{dt} = \int_0^z dz\, \frac{dV(z)}{dz} \frac{R_{\rm GRB}(z)}{1+z}, \tag{17}$$

where $R_{\rm GRB}(z)$ is the comoving GRB rate density and $dV(z)/dz$ is the isotropic comoving volume element,

$$\frac{dV}{dz} = 4\pi \left[\int_0^z \frac{dz'}{\sqrt{\Omega_M (1+z')^3 + \Omega_\Lambda}}\right]^2 \frac{1}{\sqrt{\Omega_M (1+z)^3 + \Omega_\Lambda}}. \tag{18}$$

We assume $R_{\rm GRB}(z) \propto R_{\rm SN}(z) \propto R_{\rm SF}(z)$, where $R_{\rm SN}(z)$ and $R_{\rm SF}(z)$ are the comoving rate densities of core-collapse supernovae and star formation, respectively (Porciani & Madau 2001). We also assume a constant fraction $k = R_{\rm GRB}/R_{\rm SN} \sim 10^{-5}$, which considers the GRB formation efficiency out of the core-collapse SNe and the GRB beaming effect. In addition, we take $R_{\rm SN}(z) \simeq 0.01 R_{\rm SF}(z)\ M_\odot^{-1}$. The global star formation rate for the Einstein–de Sitter universe (Steidel et al. 1999) is

$$R_{\rm SF}(z) = 0.16 \frac{\exp(3.4z)}{\exp(3.4z) + 22}\ M_\odot\ {\rm yr}^{-1}\ {\rm Mpc}^{-3}. \tag{19}$$

Thus, we derive the detection probability of low-z GRBs in the *Swift* era (2–4 yr): when $z \leq 0.1$, there will be <1 burst, and when $z \leq 0.2$, there will be a few bursts. These results agree with the present observational GRB data. In addition, taking into account possible different origins of very low-z bursts (e.g., GRB 980425) and high-z bursts, it might not be valid to directly apply the low-z calibrated relation to a high-z sample. However, if the cosmic evolution of the "standard candle" relation is ignored, then in the future one could consider a sample of GRBs with redshift $z \leq 0.2$ for the low-z calibration. As the zero-order approximation, the theoretical luminosity distance of such a GRB sample can be written as $d_L(z) = z(c/H_0)$.

5. CONCLUSIONS AND DISCUSSION

At present, GRBs with known redshifts are about 45 out of a few thousands, among which 17 are available to derive the Ghirlanda relation. This relation is so tight that it has been considered for cosmological use. Although the low-z calibration of the Ghirlanda relation is not realized, the observed 17 high-z bursts still provide interesting and even inspiring results. We find that GRBs independently place a constraint on the mass density $0.16 < \Omega_M < 0.45$ (1 σ) for a flat ΛCDM model.

GRBs are becoming more and more standardized candles. Through the Ghirlanda relation, the mean scatter in GRBs is a factor of $\sim$2 larger than that in SNe Ia. However, the disadvantage of larger scatter in GRBs is compensated, to some extent, by their advantages of high redshifts and immunity to the dust extinction. The shape of the constraints in Figure 6 implies that GRBs could not only measure the mass density Ω_M but also provide complementarity to SN cosmology. The *Swift* satellite will hopefully establish a large GRB sample with known redshifts, perhaps including low-z bursts. In this sense, GRB cosmology now lies in its babyhood.

A reliable theoretical basis of the Ghirlanda relation is also important for GRBs as a cosmic ruler. Using the small-angle approximation for all bursts, a scaling analysis gives $E_\gamma \propto E_p^a$ ($a \sim 1.5$) as long as the parameters such as the spectral index p of the distribution of accelerated electrons, the energy equipartition factor ϵ_e of the electrons, the energy equipartition factor ϵ_B of the magnetic field, the bulk Lorentz factor γ, etc., or their combinations are clustered (Zhang & Mészáros 2002; Dai & Lu 2002; Wu et al. 2004). This power-law relation could also be understood by the emissions from off-axis relativistic jets (Yamazaki et al. 2004; Eichler & Levinson 2004; Levinson & Eichler 2005) and the dissipative photosphere model (Rees & Mészáros 2005). Different plausible explanations imply that this topic needs further investigations.

It should be pointed out that the Ghirlanda relation is obtained under the framework of the uniform top-hat jet model. Other input assumptions include the uniform circumburst medium density n and the constant efficiency η_γ of converting the initial ejecta's kinetic energy into gamma-ray energy release. However, n and η_γ should be different from burst to burst, and n is variable for a burst in the wind environment (Dai & Lu 1998; Chevalier & Li 1999). Thus, the quantity $n\eta_\gamma$ in the Ghirlanda relation might not be clustered for the observed bursts (FB05). New relations with as few well-observed quantities as possible are required for improvement.[5] In this paper, for those bursts with unknown n, we assumed $n \simeq 3\ {\rm cm}^{-3}$ as the median value of the distribution of the measured densities, together with a constant fractional uncertainty of 80% (Ghirlanda et al. 2004a; DLX04). We also treat $\eta_\gamma = 0.2$ and $\sigma_{\eta_\gamma} = 0$ for all the 17 bursts.

Finally, the Ghirlanda relation is not valid for all of the observed BATSE (Burst and Transient Source Experiment) sample. This implies that this relation may suffer from the data selection effect (Band & Preece 2005). Its validity will be tested by the ongoing observations of the *Swift* mission. However, no matter whether the low-z sample is established or not, GRB cosmology is expected to progress much in the coming years.

X. D. is grateful to X. L. Luo for helpful discussions. We thank the anonymous referees for valuable comments that have allowed us to improve our paper significantly. This work was supported by the National Natural Science Foundation of China (grants 10233010, 10221001, and 10463001), the Ministry of Science and Technology of China (NKBRSF G19990754), the National Postdoctoral Foundation of China, and the Research Foundation of Guangxi University.

[5] After the submission of this paper, Liang & Zhang (2005) and Xu (2005) proposed new relations between the isotropic gamma-ray energy and the νF_ν peak energy by considering the break time of an afterglow light curve. Clearly, these three quantities are directly observed.

REFERENCES

Allen, S. W., Schmidt, R. W., Fabian, A. C., & Ebeling, H. 2003, MNRAS, 342, 287
Amati, L. 2003, Chinese J. Astron. Astrophys. Suppl., 3, 455
Amati, L., et al. 2002, A&A, 390, 81
Andersen, M. I., Masi, G., Jensen, B. L., & Hjorth, J. 2003, GCN Circ. 1993, http://gcn.gsfc.nasa.gov/gcn/gcn3/1993.gcn3
Band, D. L., & Preece, R. D. 2005, ApJ, 627, 319
Band, D. L., et al. 1993, ApJ, 413, 281
Barraud, C., et al. 2003, A&A, 400, 1021
Barth, A. J., et al. 2003, ApJ, 584, L47
Bennett, C. L., et al. 2003, ApJS, 148, 1
Berger, E., et al. 2002, ApJ, 581, 981
———. 2003, Nature, 426, 154
Björnsson, G., Hjorth, J., Jakobsson, P., Christensen, L., & Holland, S. 2001, ApJ, 552, L121
Bloom, J. S., Frail, D. A., & Kulkarni, S. R. 2003, ApJ, 594, 674
Bloom, J. S., Frail, D. A., & Sari, R. 2001, AJ, 121, 2879
Bromm, V., & Loeb, A. 2002, ApJ, 575, 111
Carroll, S. M., Press, W. H., & Turner, E. L. 1992, ARA&A, 30, 499
Chevalier, R. A., & Li, Z. Y. 1999, ApJ, 520, L29
Ciardi, B., & Loeb, A. 2000, ApJ, 540, 687
Crew, G. B., et al. 2003, ApJ, 599, 387
Dai, Z. G., Liang, E. W., & Xu, D. 2004, ApJ, 612, L101 (DLX04)
Dai, Z. G., & Lu, T. 1998, MNRAS, 298, 87
———. 2002, ApJ, 580, 1013
Djorgovski, S. G., Frail, D. A., Kulkarni, S. R., Bloom, J. S., Odewahn, S. C., & Diercks, A. 2001, ApJ, 562, 654
Djorgovski, S. G., Kulkarni, S. R., Bloom, J. S., Goodrich, R., Frail, D. A., Piro, L., & Palazzi, E. 1998, ApJ, 508, L17
Eichler, D., & Levinson, A. 2004, ApJ, 614, L13
Fenimore, E. E., & Ramirez-Ruiz, E. 2000, preprint (astro-ph/0004176)
Firmani, C., Ghisellini, G., Ghirlanda, G., & Avila-Reese, V. 2005, MNRAS, 360, L1 (FGGA05)
Frail, D. A., Waxman, E., & Kulkarni, S. R. 2000, ApJ, 537, 191
Frail, D. A., et al. 2001, ApJ, 562, L55
———. 2003, ApJ, 590, 992
Friedman, A. S., & Bloom, J. S. 2005, ApJ, 627, 1 (FB05)
Galama, T. J., et al. 1998, ApJ, 497, L13
Ghirlanda, G., Ghisellini, G., & Lazzati, D. 2004a, ApJ, 616, 331
Ghirlanda, G., Ghisellini, G., Lazzati, D., & Firmani, C. 2004b, ApJ, 613, L13 (GGLF04)
Gou, L. J., Mészáros, P., Abel, T., & Zhang, B. 2004, ApJ, 604, 508
Greiner, J., Guenther, E., Klose, S., & Schwarz, R. 2003a, GCN Circ. 1886, http://gcn.gsfc.nasa.gov/gcn/gcn3/1886.gcn3
Greiner, J., Peimbert, M., Estaban, C., Kaufer, A., Jaunsen, A., Smoke, J., Klose, S., & Reimer, O. 2003b, GCN Circ. 2020, http://gcn.gsfc.nasa.gov/gcn/gcn3/2020.gcn3
Halpern, J. P., et al. 2000, ApJ, 543, 697
Hjorth, J., et al. 2003, ApJ, 597, 699
Holland, S. T., et al. 2002, AJ, 124, 639
———. 2003, AJ, 125, 2291
———. 2004, AJ, 128, 1955
Jakobsson, P., et al. 2003, A&A, 408, 941
———. 2004, A&A, 427, 785
Jimenez, R., Band, D. L., & Piran, T. 2001, ApJ, 561, 171
Klose, S., et al. 2004, AJ, 128, 1942
Kulkarni, S. R., et al. 1999, Nature, 398, 389
Lamb, D. Q., & Reichart, D. E. 2000, ApJ, 536, 1
Lamb, D. Q., et al. 2004, NewA Rev., 48, 423
Le Floc'h, E. 2002, ApJ, 581, L81
Levinson, A., & Eichler, D. 2005, ApJ, 629, L13
Liang, E. W., Dai, Z. G., & Wu, X. F. 2004, ApJ, 606, L29
Liang, E. W., & Zhang B. 2005, ApJ, 633, 611
Lloyd-Ronning, N. M., & Petrosian, V. 2002, ApJ, 565, 182
Lloyd-Ronning, N. M., & Ramirez-Ruiz, E. 2002, ApJ, 576, 101
MacFadyen, A. I., & Woosley, S. E. 1999, ApJ, 524, 262
Masetti, N., et al. 2000, A&A, 354, 473
Matheson, T., et al. 2003, ApJ, 582, L5
Norris, J. P., Marani, G. F., & Bonnell, J. T. 2000, ApJ, 534, 248
Panaitescu, A., & Kumar, P. 2002, ApJ, 571, 779
Perlmutter, S., et al. 1999, ApJ, 517, 565
Piro, L., et al. 2000, Science, 290, 955
Porciani, C., & Madau, P. 2001, ApJ, 548, 522
Press, W. H., et al. 1999, Numerical Recipes in Fortran (Cambridge: Cambridge Univ. Press)
Price, P. A., et al. 2003a, ApJ, 589, 838
———. 2003b, Nature, 423, 844
Rees, M. J., & Mészáros, P. 2005, ApJ, 628, 847
Rhoads, J. E. 1999, ApJ, 525, 737
Riess, A. G., et al. 1998, AJ, 116, 1009
———. 2004, ApJ, 607, 665
Rol, E., Vreeswijk, P., & Jaunsen, A. 2003, GCN Circ. 1981, http://gcn.gsfc.nasa.gov/gcn/gcn3/1981.gcn3
Sakamoto, T., et al. 2004, ApJ, 602, 875
———. 2005, ApJ, 629, 311
Sari, R., Piran, T., & Halpern, J. P. 1999, ApJ, 519, L17
Sazonov, S. Y., Lutovinov, A. A., & Sunyaev, R. A. 2004, Nature, 430, 646
Schaefer, B. E. 2003, ApJ, 583, L67 (S03)
Schmidt, B. P., et al. 1998, ApJ, 507, 46
Soderberg, A. M., et al. 2004, Nature, 430, 648
Spergel, D. N., et al. 2003, ApJS, 148, 175
Stanek, K. Z., Garnavich, P. M., Kaluzny, J., Pych, W., & Thompson, I. 1999, ApJ, 522, L39
Steidel, C. C., Adelberger, K. L., Giavalisco, M., Dickinson, M., & Pettini, M. 1999, ApJ, 519, 1
Tegmark, M., et al. 2004, Phys. Rev. D, 69, 103501
Tiengo, A., Mereghetti, S., Ghisellini, G., Rossi, E., Ghirlanda, G., & Schartel, N. 2003, A&A, 409, 983
Vanderspek, R., et al. 2004, ApJ, 617, 1251
Vreeswijk, P. M., Fruchter, A., Hjorth, J., & Kouveliotou, C. 2003, GCN Circ. 1785, http://gcn.gsfc.nasa.gov/gcn/gcn3/1785.gcn3
Vreeswijk, P. M., et al. 2001, ApJ, 546, 672
Wu, X. F., Dai, Z. G., & Liang, E. W. 2004, ApJ, 615, 359
Xu, D. 2005, ApJ, submitted (astro-ph/0504052)
Yamazaki, R., Ioka, K., & Nakamura, T. 2004, ApJ, 606, L33
Yonetoku, D., Murakami, T., Nakamura, T., Yamazaki, R., Inoue, A. K., & Ioka, K. 2004, ApJ, 609, 935
Zhang, B., & Mészáros, P. 2002, ApJ, 581, 1236